

Rate of Imidization of Polymerizable Reaction Mixtures: PMR-15

JUDE O. IROH, KELVIN JORDAN

Department of Materials Science and Engineering, University of Cincinnati, Cincinnati, Ohio 45221-0012

Received 5 December 1996; accepted 21 May 1997

ABSTRACT: Imidization of PMR-15 was investigated using Fourier transform infrared spectroscopy (FTIR) as a function of time and temperature. Imidization was performed at $65 \leq T \leq 300^\circ\text{C}$ for $3 \leq t \leq 150$ min. FTIR spectroscopy showed that imidization (measured by the changes in the imide carbonyl absorption at 1778 cm^{-1}) increased with temperature and time. Imidization was found to be nearly completed in 2.5 h at 300°C . Imidization of PMR-15 occurred in *three* stages: (i) the initial imidization region characterized by gradual reaction followed by (ii) a very rapid reaction region that spans about 0.5 h and (iii) a final imidization region characterized by a gradual reaction and spans about 2 h. An Avrami-type kinetic analysis was used to obtain the reaction order of 1.5 and 1.7 and the rate constant for imidization of 1.3×10^{-3} and $1.5 \times 10^{-3}\text{ min}^{-3/2}$ at 135 and 165°C , respectively. Comparison with other kinetic models shows agreement at low conversions ($p \leq 15\%$). At high conversions of $p > 20\%$, a second-order kinetic model seems to fit the data reasonably well in agreement with the observed 3/2 order. © 1997 John Wiley & Sons, Inc. *J Appl Polym Sci* **66**: 2529–2538, 1997

Key words: thermal imidization; kinetics; polyimide; rate constants; apparent activation energy

INTRODUCTION

Polyimides offer excellent thermal and mechanical stability, low dielectric constant, and chemical resistance, which make them very attractive for electronics and structural composite applications. In the electronics industry, they are used as insulation between electrically conductive layers of copper in printed wiring boards and as adhesives and passivants in corrosion control. Polymerizable reactive mixtures (PMR), polyimide is one of a variety of thermosetting polymers used in high-temperature environments ($T_g \sim 300\text{--}430^\circ\text{C}$). They are reasonably easy to process and are used as matrix resins in advanced fiber-reinforced composites. PMR-15 is one of the leading matrix res-

ins, developed by NASA for high-temperature composites. It is synthesized by reacting the dimethyl ester of 3,3',4,4'-benzophenone tetracarboxylic acid (BTDE) with 4,4"-methylenedianiline (MDA) and 5-norbornene-2,3-dicarboxylic acid ester (NE) combined in the mol ratio of 2.087 : 3.087 : 2, respectively.

Since the introduction of PMR-15, the number of applications has increased. Also, research and development designed to optimize the processing and properties of the polyimide have received increased attention. Investigators have studied the mechanical and physical properties and the effects of prolonged exposure in adverse environments on the properties of advanced fiber-reinforced composites.¹⁻⁵ However, additional investigation is needed on the kinetics of the thermal imidization of PMR-15. A number of researchers have used quantitative and qualitative vibration infrared spectroscopy as a means of determining the reactions and composition changes, which oc-

Correspondence to: J. O. Iroh.

Journal of Applied Polymer Science, Vol. 66, 2529–2538 (1997)
© 1997 John Wiley & Sons, Inc. CCC 0021-8995/97/132529-10

cur during imidization.⁶⁻¹¹ From the investigation of time- and temperature-dependent intensity changes of specific absorption bands, one can reasonably deduce possible reaction mechanisms and kinetic information such as the reaction rates and rate constants. Qualitative information can be obtained from the assignment of intermediate and final reaction products, while quantitative evaluation of the IR spectra recorded as a function of time and temperature provides the basis for the determination of the reaction kinetics. The apparent activation energy for imidization can also be obtained from temperature- and time-dependent intensity changes.

Several techniques have been employed in the characterization of the cure reaction of polyimides and the effects of thermal imidization on neat polyimide resins.⁶⁻¹¹ Hay et al.⁷ and Ginsburg and Susko⁸ used FTIR and NMR to investigate the curing and polymerization mechanisms of PMR-15. Hay et al. studied the competing reactions due to the thermal imidization conditions, which lead to variations in the prepolymer structure and molecular weight. Ginsburg and Susko studied and characterized the degree of cure by quantifying the degree of conversion of polyamic acid to polyimide. In their respective approaches, they monitored changes in the IR intensities that occurred during thermal imidization by examining the imide, anhydride, and amide absorption bands as a function of imidization temperature and time. Hay et al. determined several key implications for the processing of high-quality reproducible laminates, while Ginsburg and Susko determined the relationship between the degree of cure and the etchability of films. Ginsburg and Susko also determined, using the absorption band ratio method, that imidization was completed after approximately 1 h of aging at 130°C. Navarre⁹ investigated the curing of PMR-15 by FTIR and DSC. He showed that the curing of PMR-15 obeyed a first-order kinetic law and also reported that imidization occurred between 100 and 250°C. In this study, we report our additional findings on the effects of temperature on the kinetics of thermal imidization of PMR-15 polyimide using FTIR. Additionally, we describe the imidization of PMR-15 by an Avrami-type kinetic model.

EXPERIMENTAL

Materials

PMR-15 resin containing 50 wt % *N*-methylpyrrolidone (NMP) was purchased from Daychem

Laboratories, Dayton, OH, and used as-received. The 25 mm potassium bromide crystals, reagent-grade (KBr) powder, and spectroscopic-grade dimethylformamide (DMF) used in the IR analysis were purchased from Aldrich Chemical Co.

Isothermal Imidization

Approximately 0.7 g of the monomer mixture (as-received neat resin) was placed on tempered watch glasses and isothermally reacted at 65, 95, 135, 165, and 200°C for periods ranging from 0.05 to 2.5 h in a NAPCO 5831 vacuum oven. A small quantity of the sample aged at 200°C ($t = 1, 1.5,$ and 2.5 h) were further aged at 300°C for 2.5 h. The oven temperature was allowed to reach equilibrium and then was maintained for 0.5 h, prior to insertion of the samples. The weight of the resin was determined before and after the reaction using an analytical balance. The weight loss of the resin, ΔW was computed as the difference between the initial, W_0 , and final, W , weights of the resin, i.e., $W_0 - W = \Delta W$.

Differential scanning calorimetry (DSC) was performed by using a Polymer Laboratories Rheometric Scientific instrument. About 7–8 mg of the aged samples was scanned between 30 and 300°C, using a heating rate of 10°C/min in a nitrogen atmosphere. The thermograms were used to determine the reaction temperatures and to monitor the progress of the reactions such as the amidization, polymerization, and imidization.

IR Spectroscopy

FTIR specimens were prepared by two different methods: First, KBr powder was combined with 1 wt % of the aged resin sample and pressed to form a KBr disc. This method was used in preparing FTIR specimens from samples aged between $65 \leq T \leq 200^\circ\text{C}$. Second, for all samples aged at $T > 200^\circ\text{C}$, about 1 wt % of the as-received resin was dissolved in DMF. Three drops of the solution were placed onto 25 mm KBr windows and subsequently aged under specified conditions. A thin film of the aged polyimide left on the surface of the crystal window was used for IR spectroscopy. IR analysis was performed in the transmission mode using a Perkin-Elmer Fourier transform infrared (FTIR) spectrometer with a resolution of 4 cm^{-1} and scanned between 4000 and 400 cm^{-1} . The spectra obtained were then base-line-corrected using a multipoint leveling technique.

Table I Percent Weight Loss Data for Aged PMR-15 Neat Resin

Time (min)	Aging Temperature					
	65°C	95°C	135°C	165°C	200°C	300°C
30	29.57	33.65	40.78	42.33	42.36	—
60	25.06	33.40	36.67	42.21	42.60	42.62
90	27.22	33.34	39.05	42.70	43.50	43.53
150	28.65	33.60	38.73	42.51	43.70	43.71

RESULTS AND DISCUSSION

Weight Loss Analysis

Table I shows the dependence of the weight loss of the aged neat resin on the reaction temperature and time. The percent weight loss of the resin due to imidization increased with temperature and time. It is believed that most of the solvent (methanol) (~ 50 wt %) was removed after about 0.5 h of imidization at 135°C. Additional weight loss of the resin system, ≤ 3 wt %, occurred at longer imidization times $t \geq 1$ h. It can be seen that at shorter reaction times ($t \leq 0.5$ h) the rate of weight loss is substantially high and of about 170 and 164%/h at 200 and 135°C, respectively. At longer reaction times ($t \sim 2.5$ h), the rate of weight loss is significantly lowered to 35 and 33%/h at 200 and 135°C, respectively (Table I). This weight loss trend is associated with the initial rapid removal of methanol (solvent) and the expulsion of condensed water (during amidization and imidization). Ring closure during imidization and the loss of large amounts of solvent in the early stages of the reaction result in increased viscosity of the resin and, consequently, lowers the rate of further imidization. Any solvent that is trapped in the partially imidized and highly viscous resin may be hard to remove. It is believed that at intermediate-to-long reaction times the rate of imidization would decrease with increased aging time because of the increased viscosity of the resin. Observation of the progress of the imidization vs. time curve (Fig. 8) shows three distinct regions, corresponding to an initial slow imidization followed by a region of very rapid reaction and ending in a final region of slow imidization. Note that the maximum rate of imidization (170%/h) occurred at a short reaction time of $t \sim 0.5$ h at 200°C as shown in Table I. A variety of competing reactions including amidization, polymerization, and imidization can occur at short reaction times. At longer reaction times, imidization is the dominant process (especially at T

$\geq 165^\circ\text{C}$). Imidization is, however, hindered by diffusion effects (increased viscosity of the resin) which decrease the ability of the chains to diffuse to the reaction site, thereby reducing the rate of ring closure (imidization) and resulting in the leveling-off or gradual decrease of the imidization with time (slope of conversion curves in Fig. 8). The completion of the imidization of samples previously aged at 200°C was achieved by subsequent imidization at 300°C for 2.5 h.

Thermal Analysis

The DSC thermogram of the as-received neat resin is presented in Figure 1. Characteristic endothermic peaks were observed up to 150°C in the neat as-received resin. After aging at $T = 95^\circ\text{C}$ for $t \geq 1.5$ h, the low-temperature endothermic peaks disappeared, while new and broad peaks appeared at approximately 185 and 250°C. The endothermic peaks, which appeared around 83 and 105°C (see Fig. 1), are due to solvent (methanol) removal and a condensation reaction (amidization), which releases water. The endothermic peaks occurring at 123–150°C are due to polymerization (formation of polyamic acid) and imidization. Water is also released during polymerization and imidization. The conversion of polyamic acid to polyimide is nearly completed after about 2.5 h of reaction at 200°C [Fig. 1(b)]. The glass transition temperature, T_g , of the resin imidized at 175°C for 2 h in a N_2 atmosphere is about 320°C (Fig. 2).

IR spectroscopy was used to monitor the extent of imidization as a function of time and temperature. The IR spectra of polyimides show characteristic amide I absorption around 1660 cm^{-1} and imide I and II absorption around 1780 and 1376 cm^{-1} , respectively. Figures 3–6 show selected IR spectra of the aged PMR-15 neat resin as a function of both aging time and temperature. The imide I absorption peak increased with increased aging time and temperature. At 95°C and short

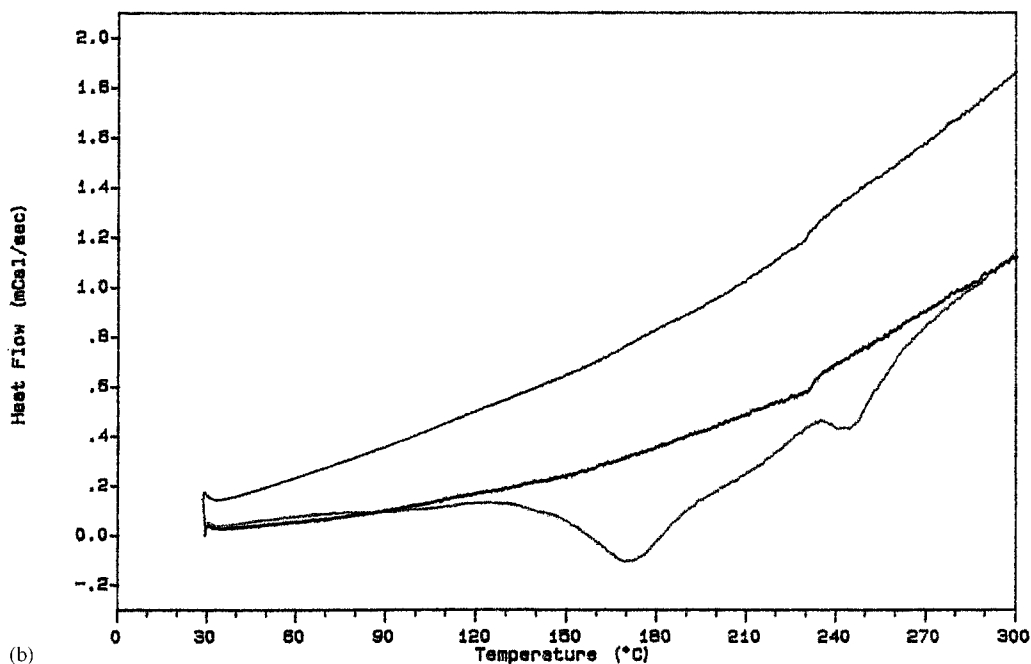
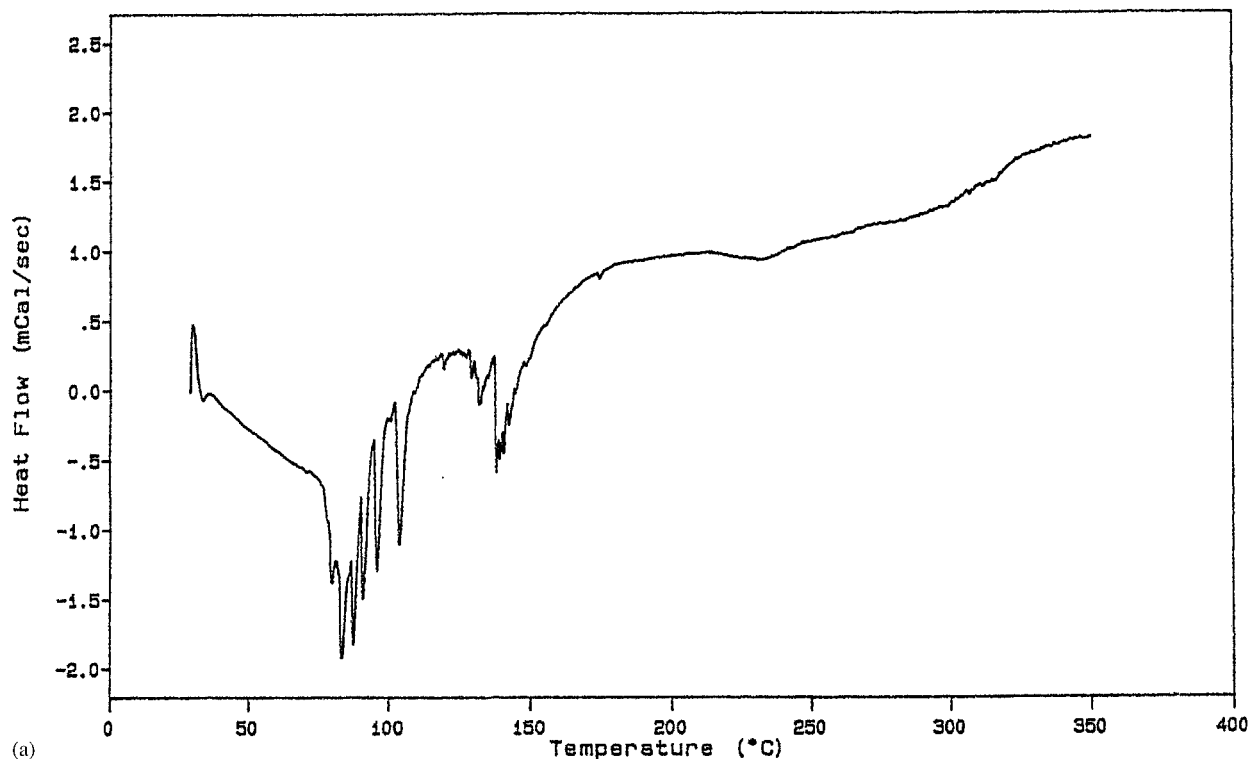


Figure 1 (a) DSC thermogram of as-received PMR-15 resin (heating rate = 10°C/min). (b) DSC thermogram of PMR-15 imidized at 95 (bottom), 165 (middle), and 200°C (top) for 2.5 h (heating rate = 10°C/min).

aging times ($t \leq 0.05$ h), a noticeable imide I peak absorption band was present, indicating that imidization had occurred (see Fig. 3). Figures 3–5 show the progress of imidization as a function

of time and temperature. Notice that anhydride formation (around 1855 cm^{-1}) occurred at higher reaction temperatures, i.e., an anhydride absorption peak was noticed at 135, 165, and 200°C after

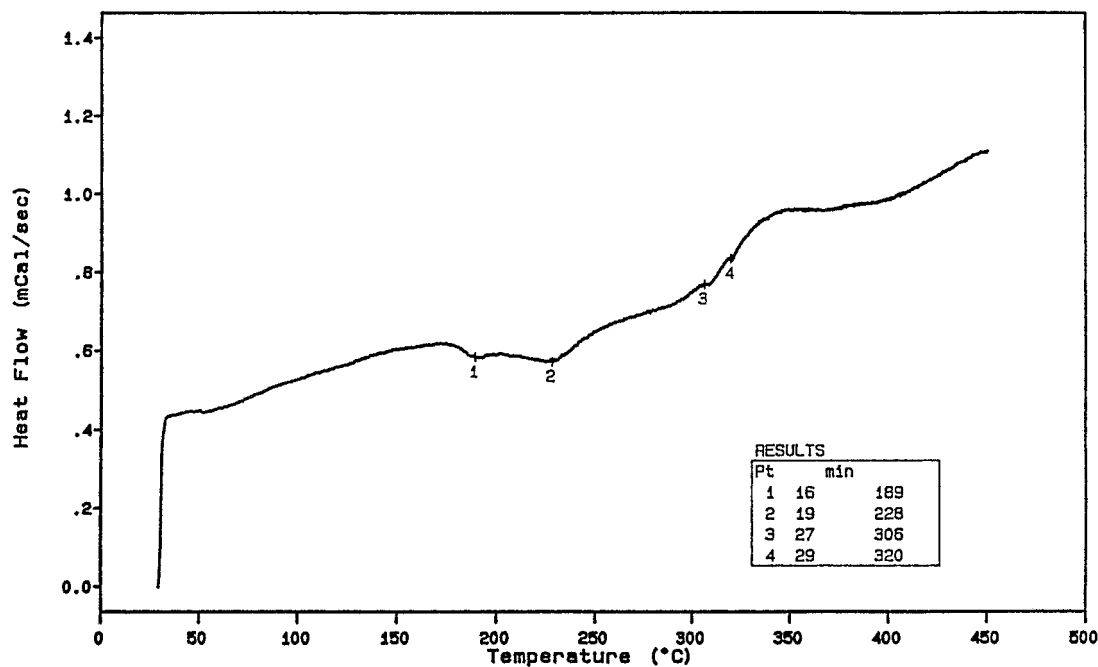


Figure 2 DSC thermogram of PMR-15 resin imidized at 175°C for 2 h in a nitrogen atmosphere (heating rate = 10°C/min).

about 0.5, 0.33, and 0.05 h of aging, respectively. Kinetic analysis performed at low conversions ($p \leq 20\%$, $t \leq 0.33$ h) and $T \leq 165^\circ\text{C}$ are not signifi-

cantly affected by anhydride formation. A significant reduction in the anhydride absorption peak occurred after additional reaction of the pre-

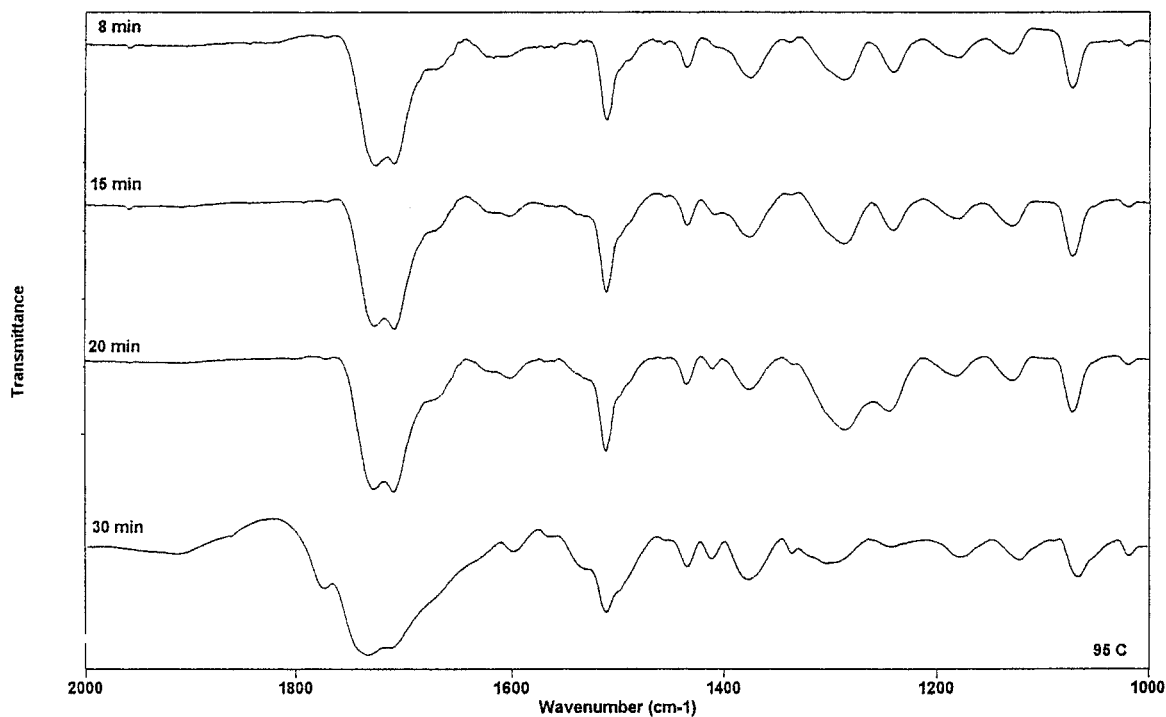


Figure 3 IR spectra of PMR-15 resin aged at $T = 95^\circ\text{C}$ as a function of time.

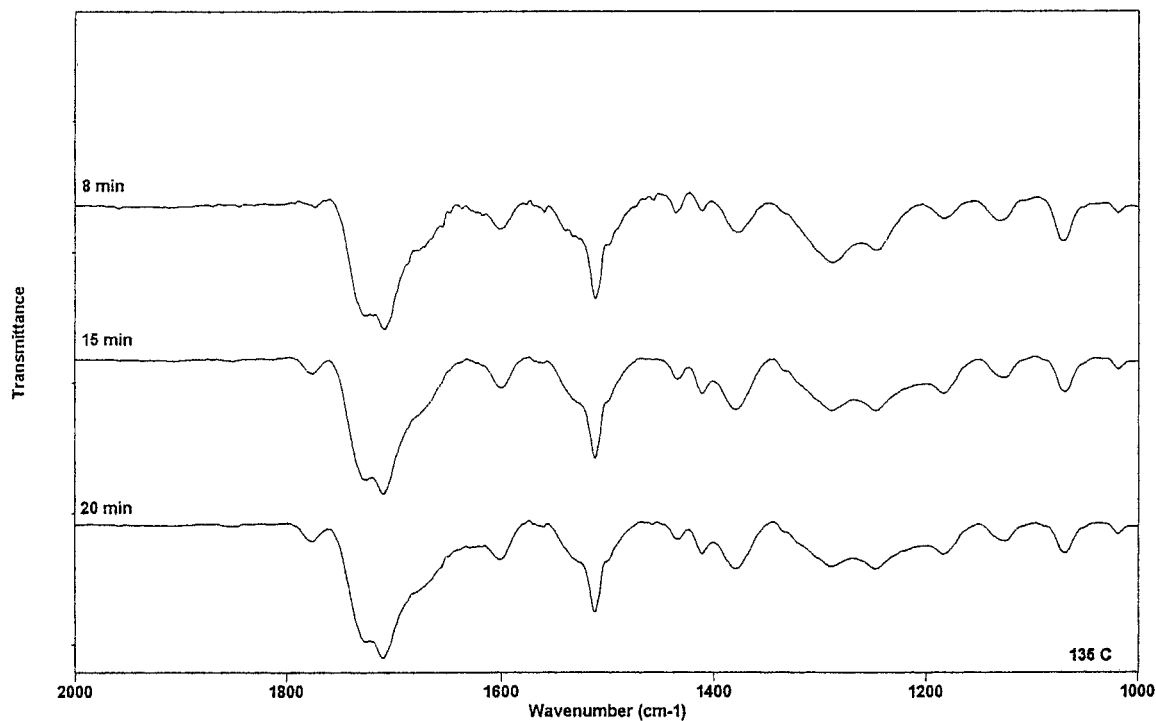


Figure 4 IR spectra of PMR-15 resin aged at $T = 135^{\circ}\text{C}$ as a function of time.

acted samples at 300°C for 2.5 h (Fig. 6). The imide absorption for the resin reacted at 200°C for 2.5 h, followed by additional aging at 300°C

for 2.5 h (Fig. 7), is approximated to the imide absorption for infinite time, i.e., $p = 100\%$. The extent of imidization (conversion) vs. time curves

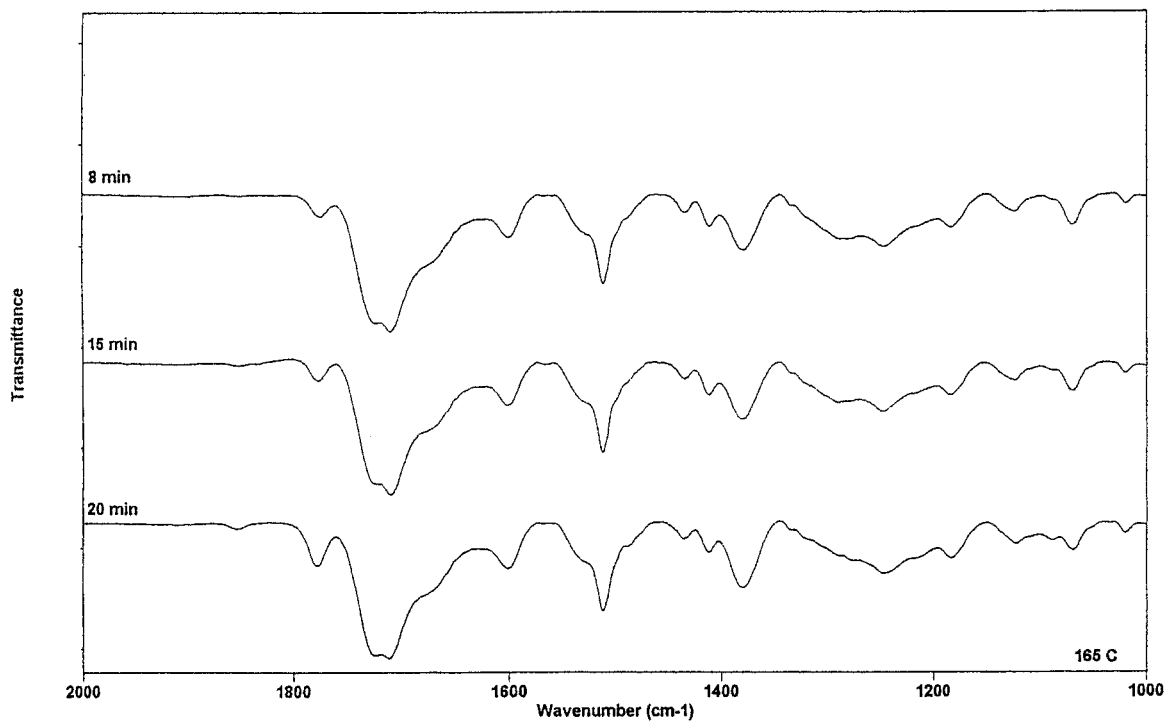


Figure 5 IR spectra of PMR-15 resin aged at $T = 165^{\circ}\text{C}$ as a function of time.

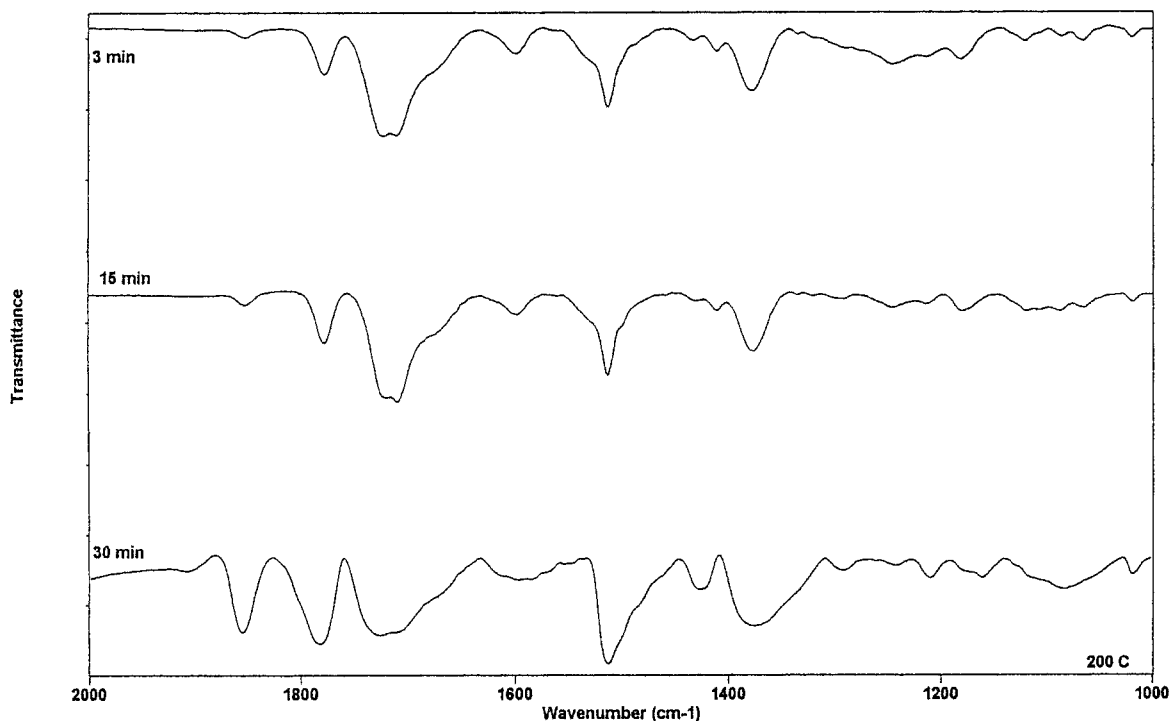


Figure 6 IR spectra of PMR-15 resin aged at $T = 200^{\circ}\text{C}$ showing anhydride formation.

(Fig. 8) show three imidization regions: (i) a slow region followed by (ii) a rapid imidization region and, finally, (iii) a gradual imidization region. In the rapid imidization region, the resin loses mobility as extensive imidization occurred, causing the T_g to exceed the reaction temperature. Plastization of the resin by the evolving solvents facilitates imidization. Imidization was followed by observing the relative increase in imide I absorption (1780 cm^{-1}) as a function of temperature and time. The peak area of the imide I, A_{1780} was normalized with that of the reference benzene ring band area at 1512 cm^{-1} , A_{1512} (benzene ring). The degree of imidization (conversion), p , was computed by using eq. (1):

$$p = \frac{\left(\frac{A_{1780}}{A_{1512}}\right)_{t,T}}{\left(\frac{A_{1780}}{A_{1512}}\right)_{t > 2.5\text{ h}, T = 300^{\circ}\text{C}}} \quad (1)$$

As shown in Figure 8, the completion of imidization takes a longer time at lower temperature. Figure 8 also resembles the nucleation and growth-type sigmoid curves comprising three dis-

tinct stages of the dehydrocyclization reaction (imidization); the initial slow reaction is followed by a rapid reaction and a final slow reaction at longer reaction times.

An attempt was made to describe the imidization of PMR-15 by using first- and second-order kinetic models. It was noted that the increase in the imide carbonyl absorption at 1780 was solely due to imidization. At short reaction times, $t \leq 20$ min ($p < 20\%$), the effect of anhydride formation is neglected. The dependence of conversion on aging time can be described by eq. (2):

$$\frac{dp}{dt} = k(1-p)^n \quad (2)$$

Integration of eq. (2) gives eq. (2b):

$$\int_{p=0}^{p=1} \frac{dp}{(1-p)} = k \int_0^t dt \quad (2a)$$

$$\text{Ln}(1-p) = kt \quad (2b)$$

where p is the degree of imidization (conversion); t , the aging time; and k , the rate constant for imidization and $n = 1$ for a first-order reaction. For n of 2 [eq. (2c)] or 3 [eq. (2d)], eq. (2b) can be rewritten as follows:

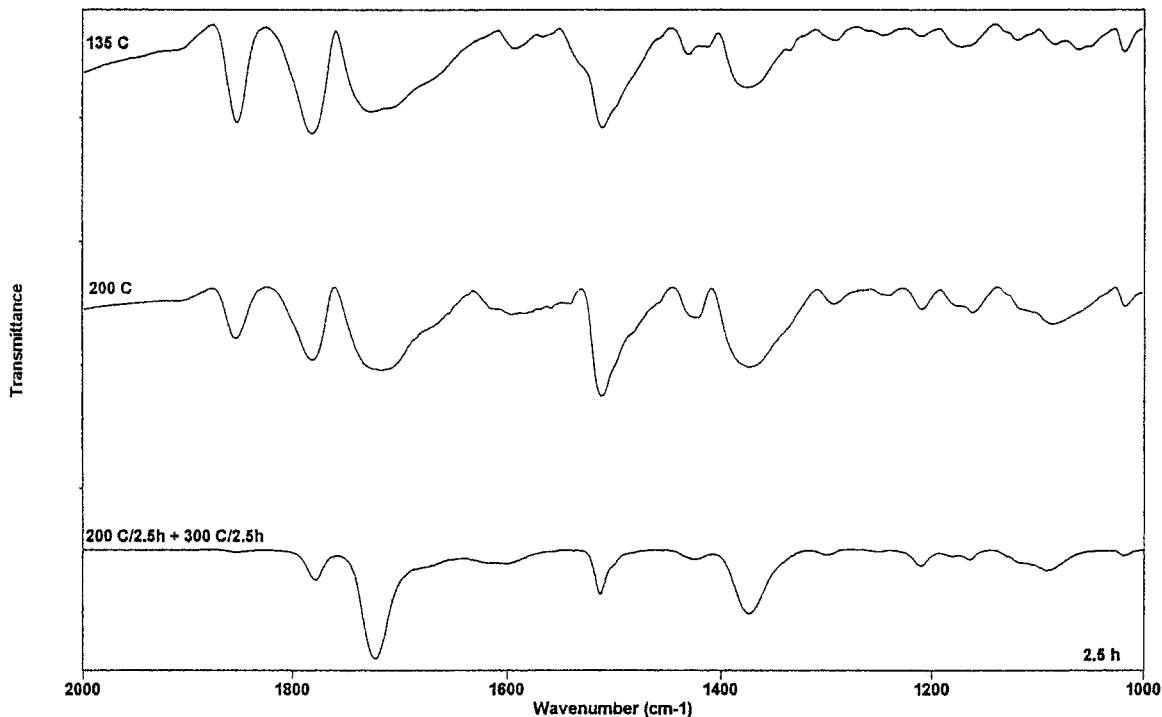


Figure 7 IR spectra of PMR-15 resin aged at $T = 200^\circ\text{C}$ for 2.5 h, followed by additional aging at 300°C for 2.5 h (bottom); aged at $T = 200^\circ\text{C}$ for 2.5 h (middle) and PMR-15 aged at $T = 135^\circ\text{C}$ for 2.5 h (top).

$$\frac{1}{1-p} = k[A]_0 t + 1 \quad (2c)$$

$$\frac{1}{(1-p)^2} = k[A]_0^2 t + 1 \quad (2d)$$

where $[A]_0$ is the initial concentration of polyamic acid. A plot of $\ln(1-p)$, $1/1-p$, and $1/(1-p)^2$

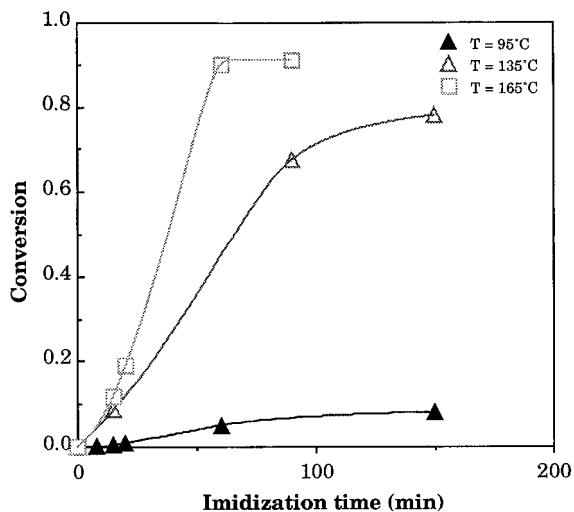


Figure 8 Effect of temperature and time on the degree of imidization.

against t [eqs. (2b), (2c), and (2d), respectively] gives k as the slope for first-, second-, and third-order reactions, respectively. k is related to the activation energy, E_a , for imidization and the frequency factor, A , as shown in eq. (3):

$$k = A \exp\left(-\frac{E_a}{RT}\right) \quad (3)$$

$$\ln k = \ln A - \frac{E_a}{RT} \quad (3a)$$

A plot of $\ln k$ against $1/T$ gives $\ln A$ as the intercept and $-E_a/R$ as the slope. Equations (2) and (3) can be combined to yield a generalized equation for imidization:

$$\frac{dp}{dt} = A \exp\left(-\frac{E_a}{RT}\right)(1-p) \quad (3b)$$

Figures 9–12 show the first- and second-order kinetic plots for imidization at 135 and 165°C . Notice that the correlation decreased at higher conversion and higher imidization temperature. A better fit was obtained using an Avrami-type

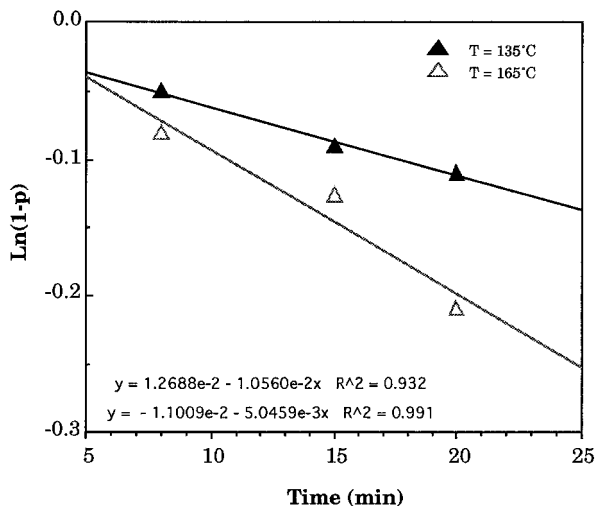


Figure 9 First-order kinetic plots for imidization of PMR-15 ($t \leq 20$ min, $T = 135$, and 165°C , $p \leq 20\%$).

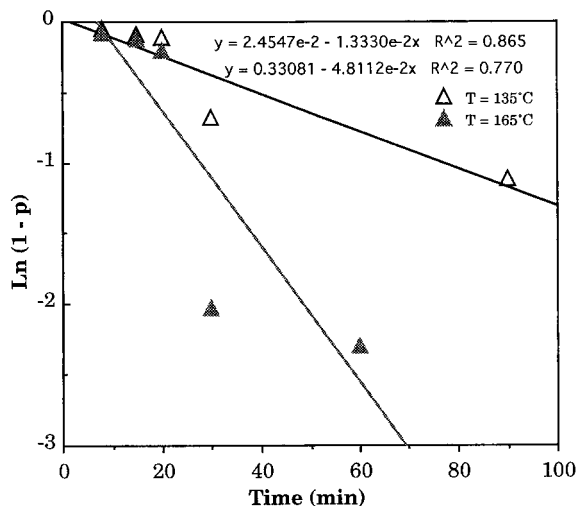


Figure 11 First-order kinetic plots for imidization of PMR-15 ($t \geq 60$ min, $T = 135$, and 165°C , $p \geq 70\%$).

double logarithmic plot, i.e., $\text{Ln}[\text{Ln}(1/1 - p)]$ vs. $\text{Ln } t$ (Fig. 13). The slope of the latter gave the order of imidization as $3/2$, while the rate constant for imidization, k , of about $0.16 - 0.0011$ was obtained from the intercept. The apparent activation energy for imidization was determined by plotting $\text{Ln } k$ against $1/T$, where k is obtained from the intercept of the Avrami plot. The activation energy of 4 kJ/mol obtained for imidization is lower than the activation energy of $32 - 63$ kJ/mol obtained using the increment in the area of the imide carbonyl peak absorption band at 1780 cm^{-1} .

CONCLUSIONS

Imidization was shown to occur in three stages: a slow reaction initial region followed by a rapid imidization region and, finally, a gradual imidization region. The transition from the rapid to the final gradual imidization region was found to occur at $t \leq 0.5$ h. An Avrami-type kinetic equation was used to describe the imidization even at high conversions ($p \geq 70\%$). The 1.5 order of imidization obtained suggests a second-order kinetics for imidization. An apparent activation energy for imidization of ~ 4 kJ/mol was obtained using the Avrami analysis.

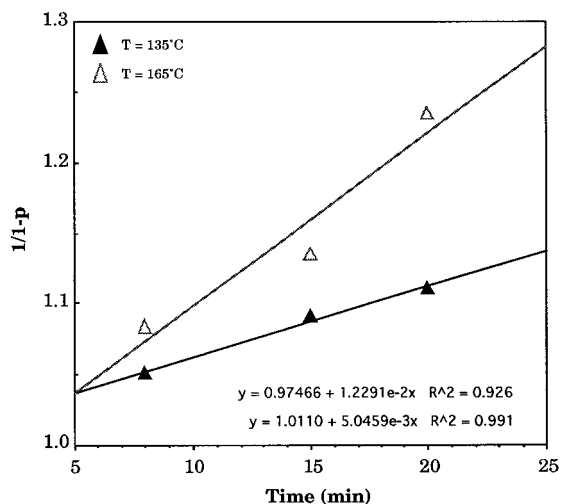


Figure 10

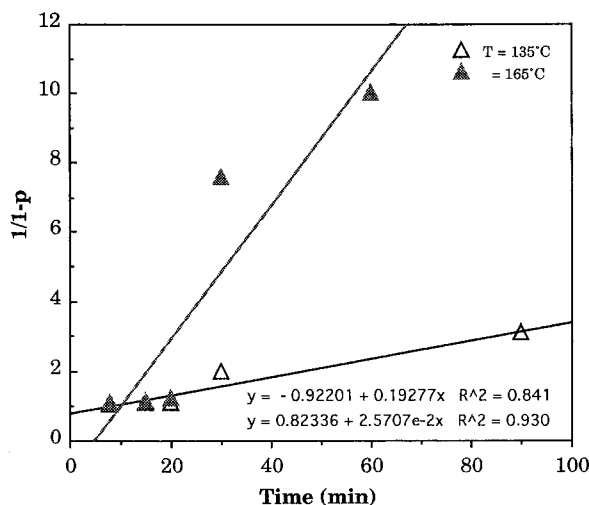


Figure 12 Second-order kinetic plots for imidization of PMR-15 ($t > 60$ min, $T = 135$, and 165°C , $p > 70\%$).

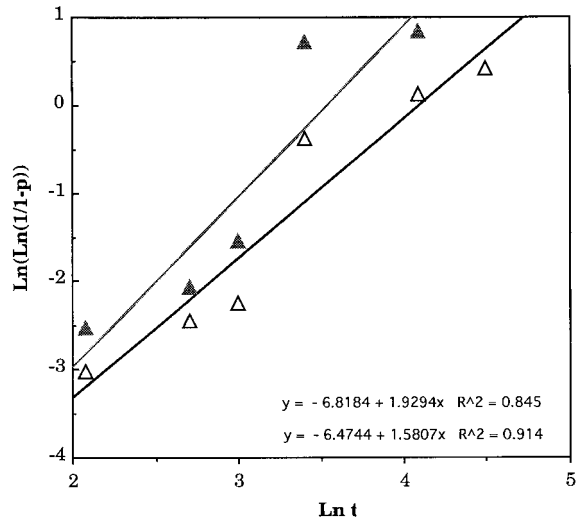


Figure 13 Avrami-type kinetic plots for imidization of PMR-15 ($t > 60$ min, $T = 135$ (bottom), and 165°C (top), $p > 70\%$).

REFERENCES

1. C. Marceau and B. Hilaire, *Polymer*, **34**, 2458–2459 (1993).
2. K. J. Bowles, D. Jayne, and T. A. Leonhardt, *SAMPE Q.*, **Jan.**, 2 (1993).
3. D. A. Scola and J. H. Vontell, *Polym. Eng. Sci.*, **31**, 6 (1991).
4. K. J. Bowles and G. Nowak, *J. Compos. Mater.*, **22**(10), 966–985 (1988).
5. K. J. Bowles, *SAMPE Q.*, **21**, 147–161 (1990).
6. K. Jordan and J. O. Iroh, *Polym. Eng. Sci.*, **36**, 2550–2555 (1996).
7. J. N. Hay, J. D. Boyle, P. G. James, J. R. Walton, and D. Wilson, *Polyimides: Materials, Chemistry and Characterization*, Elsevier, Amsterdam, 1989, pp. 305–320.
8. R. Ginsburg and J. R. Susko, in *Polyimides, Synthesis, Characterization and Applications*, K. L. Mittal, Ed., Plenum Press, New York, London, 1984, Vol. 1, pp. 237–247.
9. M. Navarre, in *Polyimides, Synthesis, Characterization and Applications*, K. L. Mittal, Ed., Plenum Press, New York, London, 1984, Vol. 1, pp. 429–442.
10. J. A. Hinkley, *J. Adv. Mater.*, **Apr.**, 55–59 (1996).
11. J. K. Choi and A. Lee, in *3rd International Conference for Composite Engineering*, New Orleans, LA, July 21–26, 1996, pp. III-A-1–III-A-10.